FATIGUE PROPERTIES AND TRIBOLOGICAL TESTS OF AISI 316 STEEL AFTER HIGH PRESSURE TORSION

Andrey Volokitin[1], Irina Volokitina[2], Abdrakhman Naizabekov[2], Dmitry Kuis[3], Sergey Lezhnev[2], Evgeniy Panin[1]

[1]*Karaganda State Industrial University*
101400, Republic av. 30, Temirtau, Kazakhstan
[2]*Rudny Industrial Institute*
111500, 50 let Oktyabrya str. 38, Rudny, Kazakhstan
[3]*Belarusian State Technological University*
220006, Sverdlova 13a, Minsk, Belarus
E-mail: irinka.vav@mail.ru

Received 01 September 2022
Accepted 27 November 2022

ABSTRACT

The influence of the high pressure torsion process in the new die on the fatigue properties of AISI 316 corrosion-resistant steel was investigated. Eight deformation cycles was carried out at cryogenic and ambient temperatures. It was revealed that the fatigue strength of both samples increases due to the structure grinding and twinning in austenite during deformation by high pressure torsion, partially martensitic transformation and an increase in the proportion of large-angle boundaries during cyclic deformation. The main factor of the higher fatigue limit of AISI 316 steel after deformation at cryogenic temperature compared to ambient temperature is a more intensive microstructure grinding and the presence of an increased proportion of large-angle boundaries and the course of a more complete martensitic transformation.

Keywords: severe plastic deformation, high pressure torsion, fatigue properties, tribology, cryogenic conditions.

INTRODUCTION

Currently, in many areas of industry, due to the growing requirements for the reliability of structures, there is a steady trend towards the introduction of materials with high indicators of both strength and plasticity. Traditional methods of increasing the strength characteristics (various methods of heat treatment or deformation hardening, including methods of severe plastic deformation) in most cases lead to a decrease in the plastic properties of materials and products made of them [1, 2]. Therefore, the construction of steels with high strength and plastic properties at the same time belongs to the most important trends of modern industry. There are many technological methods of plastic deformation of metals - various types of forging, rolling, drawing, extrusion, pressing, etc., however, not all of them can be used to disperse the structure to the nanoscale. To form an ultrafine-grained (UFG) or nanostructured (NS) state with an average grain size of about 100 nm or less, it is necessary to subject the metal to severe plastic deformation (SPD), which consists in the implementation of large deformation degrees at relatively low temperatures (below 0.3 - 0.4 of melting temperature) under high applied pressures [3 - 8]. It is known that a combination of two factors is important for obtaining UFG and NS materials: high intensity and significant non-monotonicity of deformation carried out at temperatures no higher than the temperature of the return process [9]. The first process ensures the generation of dislocations and the evolution of the dislocation structure, and the second leads to the activation of new sliding systems of lattice dislocations and their interaction with the small angle boundaries of fragments formed during deformation, which leads to their restructuring into high angle boundaries of a general type. Also, one of the conditions that ensure the production of UFG and NS materials during their plastic deformation is the presence of high hydrostatic pressure, which will prevent the formation of cracks and pores [10].

All applied SPD methods, in accordance with the

deformation scheme used, can be divided into two groups:

- not using high hydrostatic pressures, for example: multi-axis deformation (all-round forging) [11], alternating bending [12] and accumulating joint rolling [13, 14];

- using high hydrostatic pressures: high pressure torsion, screw pressing [15, 16], equal-channel angular pressing [18 - 20].

One of the most common SPD methods is equal-channel angular pressing (ECAP), the principle of which is to implement a simple shift in the channels intersection area of equal cross-section, made in a monolithic matrix and located at an angle to each other, when pushing the workpiece through them. The prevalence of this method is due to its simplicity, low specific loads on the tool and the possibility of giving the workpiece a large shear deformation due to an almost unlimited number of its repetitions [21]. A significant disadvantage of ECAP is the limitation of the transverse dimensions of the processed materials: despite the fact that there are data on obtaining samples with a diameter of more than 100 mm, with an increase in transverse dimensions, the complexity of obtaining a homogeneous nanostructure increases significantly, the material utilization factor decreases, the requirements for the power of pressing equipment and the strength of tooling sharply increase [22].

Another common SPD method is high-pressure torsion (HPT) [15]. The main advantages of the HPT method [23] are the possibility of implementing extremely high shear stresses with relatively simple tooling, even brittle materials can be deformed at low temperature. However, the prospects for using HPT as an industrial processing method have significant limitations due to the very small size of the samples - as a rule, these are thin discs with a thickness of about 1 mm and a diameter of 20 - 30 mm.

Despite the fact that SPD methods find experimental and industrial application in the procurement production of machine-building and metallurgical enterprises, which have recently been at the stage of laboratory and experimental development, at the moment there are a number of factors limiting their wide application in industry [24]. A promising direction for improving the properties of steels and alloys is the development of complex processing methods combining methods of plastic deformation and heat treatment [25 - 27].

Thus, at the moment there is a need both to improve the SPD schemes and equipment, and to develop common processing technologies to obtain a technologically simple and economical industrial method for processing metals and alloys capable of realizing high and megaplastic deformations, and thereby achieve significant dispersion of the structure of the processed material. One of such methods is the HPT in a stamp of a new design, which allows deforming ring blanks on a crank hot-stamping single-column press. Previous works have shown good results of the influence of this process on microstructural properties and mechanical characteristics [25, 28]. But the characteristics of fatigue strength, which are important criteria for assessing the stability of the structural state of the metal and its operability under cyclic loads, have not been studied.

Therefore, the purpose of this work is to study the fatigue properties and tribological tests of AISI 316 steel after high pressure torsion at cryogenic and ambient temperatures.

EXPERIMENTAL

The initial workpiece had a ring shape with a diameter of 76 mm, a width of 3.5 mm and a thickness of 3 mm. Austenitic stainless steel AISI 316 (0,08 % C; 13 % Ni; 17 % Cr; 2,0 % Mo; 0,6 % Si; 1,8 % Mn; 0,8 % Ti) was selected as the material of the workpiece because it is high-strength, corrosion-resistant, ductile and heat-resistant. The laboratory experiment was carried out on a crank hot-stamping single-column press of PB 6330-02 model with a force of 1000 kN. The number of deformation cycles was 8. The deformation was carried out in liquid nitrogen (cryogenic temperature) and for comparison at ambient temperature.

To conduct fatigue tests, test benches developed earlier at the Belarusian State Technological University (Minsk, Belarus) were used. To conduct tests at high frequencies (3; 9 and 18 kHz), magnetostrictive stands operating in self-oscillating mode were used, the schematic diagram of which is shown in Fig. 1. To establish the frequency dependence of the fatigue durability of materials, as well as the nature of changes in their physical and mechanical properties during cyclic loading, test complexes with bending and longitudinal frequencies were used fluctuations of 0.15; 3.9; 18 kHz (Fig. 2). Magnetostrictive transducers served as active

elements of these installations that convert electrical vibrations into mechanical ones. Mechanical vibrations of the package occur under the influence of an alternating magnetic field excited by high-frequency generators. The efficient operation of the converters is ensured by an optimal level of magnetization by a constant magnetic field. For stands operating at a resonant frequency of 18 kHz, standard magnetostrictive converters of the batch type PMS-15A-18, assembled from thin permendure plates, were used. For stands operating at frequencies of 3 and 9 kHz, special packages with the above resonant frequencies and original active elements made of nickel plates were used. The packages were connected by soldering with a flange made of 45 steel, which in turn was attached to the hubs by means of a threaded connection. To prevent self-unscrewing of the thread and the convenience of frequency matching of the concentrator with the converter, a special acoustic resonator is applied, pressed by springs to the free end of the active element [29].

All sizes of the elements of these oscillatory systems were performed with the same natural frequency, which made it possible to obtain maximum values of the amplitude of cyclic stresses in the sample when the installations were operating at a given resonant frequency. Calculations of magnetostrictive transducers were carried out in accordance with the methodology [29].

In order to increase the amplitude, rods of variable cross–section were attached to the packages - mechanical vibration amplifiers (concentrators), to which, in turn,

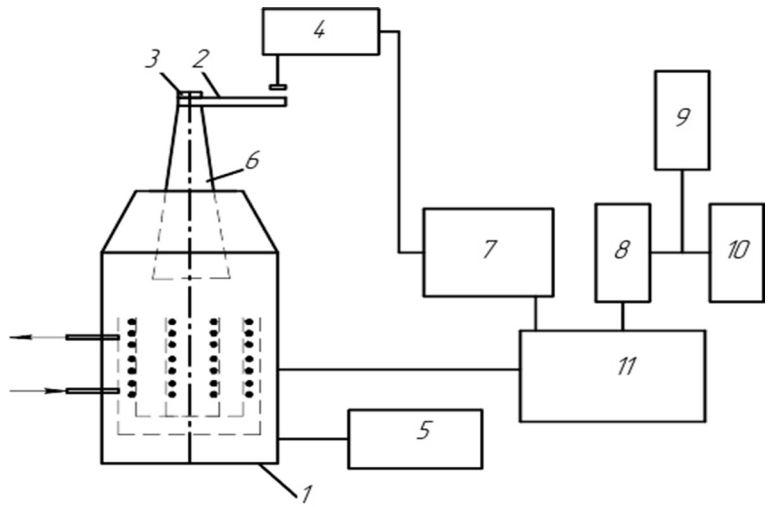

Fig. 1. Schematic diagram of the complex performing loading in a wide range of frequencies and temperatures: 1 - magnetostrictor converter; 2 - sample; 3 - mounting device; 4 - MRTI vibrometer; 5 - magnetization module; 6 - waveguide concentrator; 7 - amplitude stabilization device (ASD); 8 - frequency meter; 9 - oscilloscope; 10 - output to a PC; 11 - amplifier and signal generator.

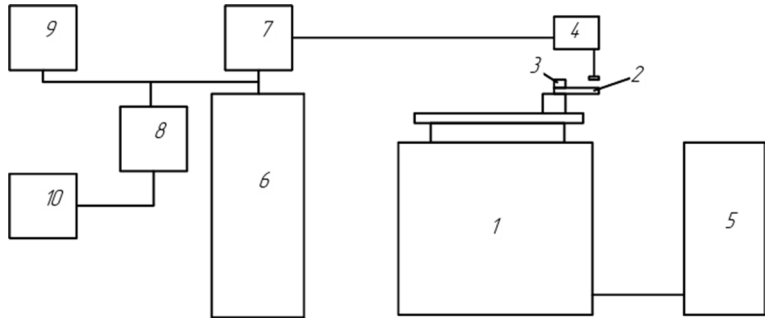

Fig. 2. Schematic diagram of a low-frequency test bench for kinematic excitation of flexural vibrations: 1 - VE vibrator; 2 - sample; 3 - mounting device; 4 - MRTI vibrometer; 5 - magnetization module; 6 - SAVAGE amplifier; 7 - amplitude stabilization device (ASD); 8 - frequency meter; 9 - oscilloscope; 10 - output to a PC.

samples were attached. Conical, stepped cylindrical and ampoule-stepped concentrators were used, and the latter type was used only in stands at loading frequencies of 3 and 9 kHz. The calculation of the concentrator elements was carried out according to the general method of calculating multistage rods.

The shape and dimensions of the sample attachment with oscillation concentrators were determined by the requirements of minimizing resonant-oscillating masses due to the limited power of experimental installations. It was found that the use of known fasteners led either to insufficient positioning accuracy of the sample, low Q-factor of the system, or they showed low reliability in operation. Their use leads to a significant increase in the dispersion of fatigue resistance characteristics, which increases the duration of tests by 2 - 3 times.

To increase the reliability of the sample attachment based on the analysis of the forces acting on its parts, a fastening device has been developed and patented (BY patent No. 12601) [30] that ensures the stability of the friction coefficient when exposed to high-frequency vibrations (18 kHz) by increasing the tightening force. The proposed design made it possible to increase the accuracy of positioning the sample relative to the concentrator due to the coaxial slots on the shank of the concentrator and the clamping sleeve. The results of comparative tests at a frequency of 18 kHz showed a decrease in the scattering of fatigue resistance characteristics by 25 % - 30 %, which made it possible to increase the accuracy and reliability of their determination, reduce the consumption of the materials under study and the complexity of the tests.

The use of the proposed design of sample attachment and the calculated dependencies for determining the stress-strain state of the samples allowed to reduce the uncertainty of finding the endurance limit by the proposed method by 20 %. At the same time, the difference with the test results obtained at a low loading frequency was no more than 10 %.

The converters were powered by high-frequency current either from an UPV-5 type amplifier (frequencies 3 and 9 kHz), or from the standard amplifier blocks of the UZG-2-4M generators (frequency 18 kHz) and UZDN-2T (frequency 44 kHz), for which their partial modernization was carried out, allowing operation in self-oscillating mode when the master generator is disabled.

One of the problems affecting the correctness of the fatigue test results is the stabilization of the oscillation amplitude during loading. This issue is particularly acute when using a resonant mode, since a change in the amplitude of the oscillations can be caused by both a change in the acoustic power supplied to the sample and a mismatch in the frequency of the mechanical resonance of an oscillatory system with an acute characteristic with the frequency of the generator current used in the circuit with independent excitation. In this regard, installations with self-oscillating mode of operation were used, allowing to study the kinetics of sample damage by changing the resonant frequency.

The test complexes operated in self-oscillating mode; the set parameters of the oscillation of the samples were maintained using a special device for stabilizing the amplitude of the PSA. Since the Q-factor of this self-oscillating system is mainly determined by the Q-factor of the sample, then during fatigue tests there is a real possibility of monitoring the kinetics of accumulation of fatigue damage by tracking the change in the frequency of vibrations of the system using an electronic frequency meter. The optimal mode of operation of the generator amplifier was provided by powering the magnetization windings of magnetostrictors with a direct current of the block. In order to avoid overheating of the active and magnetizing windings of the converters, they were cooled with running water. Preliminary adjustment and calibration of the vibrometer was carried out using an optical microscope of the MBS-2 type. The control of the shape and amplitude of electrical signals was carried out using an electronic oscilloscope connected to the circuit for the duration of the control.

To carry out fatigue tests at a low frequency of bending vibrations, a test installation based on an electrodynamic vibration stand of type B3 was used, the schematic diagram of which is shown in Fig. 2. Alternating current supply of the active coils of the type B3 vibrator table (the maximum weight of the tested parts is 20 kg) was carried out from a SAVAGE type amplifier (operating frequencies 10-5000 Hz).

When testing plate samples of complex shape with a stress concentrator to control the level of cyclic stresses, the vibration stand was additionally equipped with a TOPAZ 10 - 3 type strain booster (not shown in the diagram). The magnitude of cyclic stresses acting in the dangerous section of the sample was determined using a strain gauge glued in this section. When it failed

due to fatigue damage, further monitoring was carried out with the help of an additional load cell glued at the site of lower voltages. Otherwise, the operation of this installation did not differ from the operation of the high-frequency test complexes described above.

When upgrading to control the level of cyclic stresses, the vibration stand was additionally equipped with a multi-channel Spider-type strain booster (not shown in the diagram). The values of cyclic stresses acting both in the dangerous section of the sample and in other sections with a lower stress level were determined using strain gages glued on various sections. The use of 3 to 5 strain gages made it possible to determine the stress state of the sample with higher accuracy at different amplitudes of its oscillations.

Tribotechnical tests of coating samples were carried out on an automated ATVP tribometer equipped with a specially designed device for registering the coefficient of friction. The friction coefficient was measured at various stages of the cycle of mutual movement of the contacting bodies and during the entire test period. The measured values of the friction coefficients were statistically processed and the maximum and average values off were determined at each test cycle. The obtained values were accumulated in the operational data file of the computing device and used to construct a graphical dependence on the number of test cycles. In addition, after every 512 cycles, the values of the friction forces were recorded in detail during one loading cycle. The measurement error does not exceed 5 % of the measured value.

Tribotechnical tests of coating samples were carried out according to the scheme of reciprocating motion of contacting bodies at an average speed of mutual movement of 0.1 m/sec on an automated ATVP tribometer equipped with a specially designed device for registering the friction force and then determining the values of the friction coefficient. Comparative tests of antifriction properties of coating samples were carried out in the friction mode without lubricant (dry friction). The tested samples had the shape of a rectangular prism with the dimensions of the working surface of 6x8 mm on which experimental TiN coatings were applied. The thickness of the samples was 2 mm. The specific load of the friction tests without lubrication was 1.0 MPa. The working surface of the coated sample was not subjected to additional processing before the tests. During the tests, a counterbody made of hardened tool steel U8 (HV = 7900 - 8000 MPa) with dimensions of 2 x 40 x 90 mm was used. The surface of the steel counterbody was polished with subsequent polishing on fine abrasive paper with a grain size of M40. Before the tests, the working surfaces of the contacting bodies were degreased with alcohol, acetone and dried.

Measurement of the wear value of prismatic samples was carried out by the weight method using analytical scales ADV-200M. The measurement error of the sample mass was 0.05 mg. Wear products were carefully removed from the surface of the samples before weighing, then the samples were washed, wiped with alcohol and dried in a drying cabinet at a temperature of 100°C. After drying, the samples were weighed on ADV-200M analytical scales. Weighing of each sample was carried out at least 2 - 3 times. The tests were carried out before reaching 8000 - 10000 cycles with intermediate weighings after each 1000 - 2000 cycles. The friction path for one test cycle was 0.06 m. The total friction path during the tests was 480 - 600 m.

The measurement of linear wear was carried out using the artificial bases method, based on determining the distance from the friction surface to the bottom of the artificial recess, which naturally narrows from the surface to the bottom of the recess. The indentations on the surface were made by pressing a diamond indenter in the form of a pyramid with a square base and an angle at the apex between the opposite faces of 136°. The bottom of the recesses serves as a permanent artificial base from which the distance to the friction surface is measured. The depth of the print was calculated using the formula H = d / 7, where d is the length of the diagonal of the print. The prints were applied using a Vickers hardness tester.

RESULTS AND DISCUSSION

Fatigue tests of AISI 316 steel samples after deformation by the HPT method at cryogenic cooling and ambient temperature were carried out on the equipment described above. The results of fatigue tests during the implementation of alternating bending at a frequency of 18 kHz are shown in Figs. 3 - 5.

The presented studies have shown that the severe plastic deformation by HPT method at cryogenic temperature led to a more significant increase in the fatigue characteristics of AISI 316 steel (at different

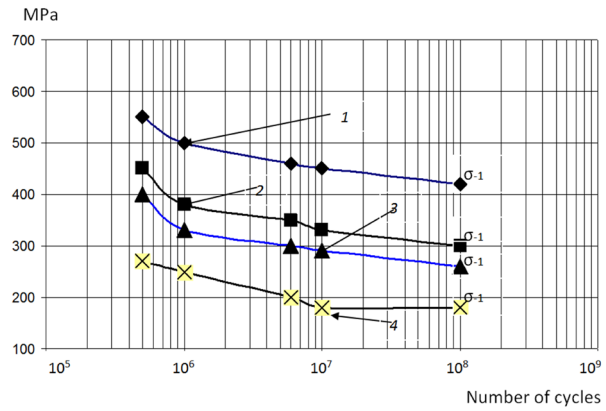

Fig. 3. Effect of HPT processing on the fatigue characteristics of AISI 316 steel at various loading levels (1,2 - loading level 254 MPa, 3,4 - loading level 346 MPa). 1, 3 - a sample deformed at cryogenic temperature, 2, 4 - a sample deformed at ambient temperature.

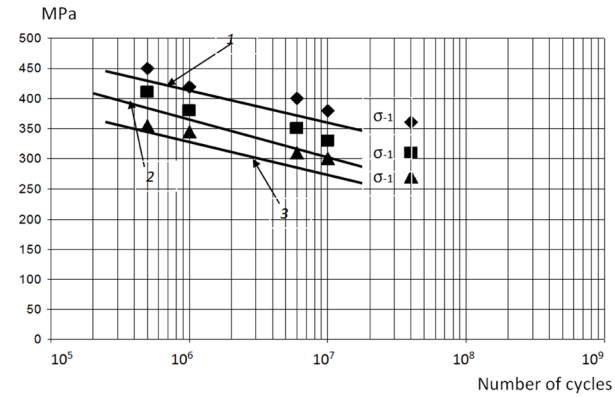

Fig. 4. Fatigue curves of AISI 316 steel after deformation by HPT method at ambient temperature at various test temperatures: 1 - 20°C, 2 - 200°C; 3 - 250°C.

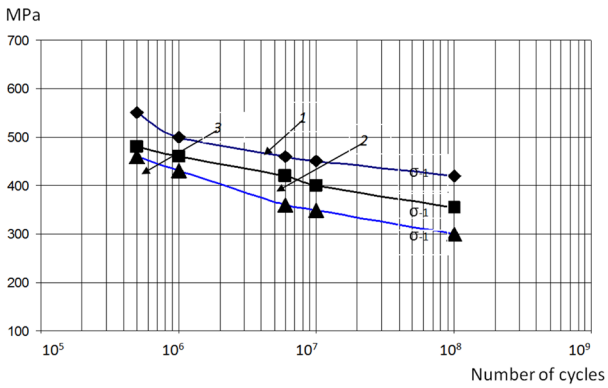

Fig. 5. Fatigue curves of AISI 316 steel after deformation by HPT method at cryogenic temperature at various test temperatures h, μm: 1 - 20°C, 2 - 200°C; 3 - 250°C.

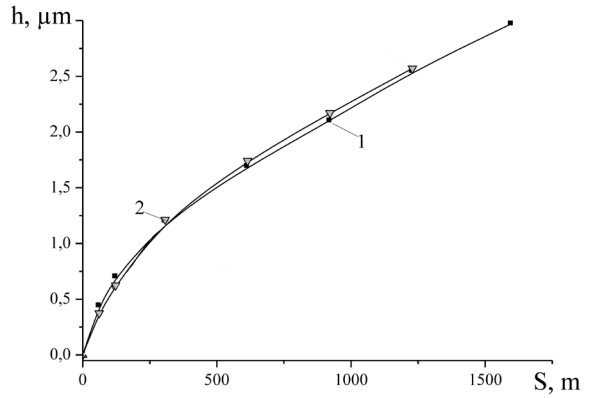

Fig. 6. Dependence of linear wear h on the friction path S (friction without lubricant, specific test load 1 MPa, counterbody - hardened steel U8): 1 - a sample deformed at cryogenic temperature; 2 - a sample deformed at ambient temperature.

temperatures and loading conditions) than when deformed at ambient temperature. At the same time, it was found that increasing the load to 346 MPa does not change the nature of fatigue curves. Such an increase in fatigue characteristics is explained primarily by obtaining a fine-grained structure as a result of severe plastic deformation by HPT method. A significant role in the fracture resistance under cyclic loading is played by a significant increase in the density of dislocations at the grain boundaries. In this case, the movement of dislocations is blocked by sliding and twinning. Thus, the process of softening of materials that precede the origin and development of a fatigue crack is significantly slowed down.

It should be noted that similar dependencies are also characteristic of elevated test temperatures (Fig. 4 and Fig. 5). An increase in temperature contributes to an earlier course of softening processes due to the activation of the interaction of dislocations and point defects, as well as the movement of dislocations.

Fig. 6 shows graphical dependences of linear wear on the friction path for a sample deformed at cryogenic temperature (curve 1) and a sample deformed at ambient temperature (curve 2). From the graphs presented in Fig. 6, it can be seen that at the initial stages of tribotechnical testing (run-in stage), the linear wear of both samples is almost the same. In this case, the value of the wear intensity for the sample deformed at cryogenic

temperature (sample 1) is $I_h = 5.7 \times 10^{-9}$, and for sample 2 - $I_h = 4.9 \times 10^{-9}$. With an increase in the duration of the tests, the wear intensity of samples 1 - 2 becomes almost the same and amounts to $I_h = 1.32 - 1.38 \times 10^{-9}$.

CONCLUSIONS

The results of the study showed that despite certain quantitative differences in the kinetics of the physical and mechanical characteristics of the AISI 316 steel material under consideration with cryogenic and ambient temperature treatment, the fatigue damage process develops according to the same patterns, characterized by a combination of hardening and softening processes. This confirms the unified physical nature of the development of fatigue damage in the considered frequency range and, consequently, the fundamental possibility of implementing accelerated fatigue tests using high loading frequencies.

Acknowledgements

This research was funded by the Science Committee of the Ministry of Education and Science of the Republic of Kazakhstan (Grant No. AP08856353).

REFERENCES

1. M. Polyakova, A. Gulin, D. Constantinov, Investigation of microstructure and mechanical properties of carbon steel wire after continuous method of deformational nanostructuring, Appl. Mechan. Mater., 436, 2013, 114-120.
2. A. Kolesnikov, R. Fediuk, M. Amran, S. Klyuev, A. Klyuev, I. Volokitina, S. Shapalov, A. Utelbayeva, O. Kolesnikova, A. Bazarkhankyzy, Modeling of Non-Ferrous Metallurgy Waste Disposal with the Production of Iron Silicides and Zinc Distillation, Materials, 15, 2022, 2542.
3. K. Muszka, D. Zych, P. Lisiecka-Graca, L. Madej, Ja. Majta, Experimental and Molecular Dynamic Study of Grain Refinement and Dislocation Substructure Evolution in HSLA and IF Steels after Severe Plastic Deformation, Metals, 10, 2020, 1122.
4. A.P. Zhilyaev, G. Ringot, Yi.Huang, J.M.Cabrera, T.G. Langdon, Mechanical behavior and microstructure properties of titanium powder consolidated by high-pressure torsion, Mater. Sci. Eng. A, 688, 2017, 498-504.
5. M. Kawasaki, B. Ahn, H.J. Lee, A.P. Zhilyaev, T.G. Langdon, Using high-pressure torsion to process an aluminum–magnesium nanocomposite through diffusion bonding, J. Mater. Res**,** 31, 2015, 88-99.
6. J. Su, D. Raabe, Z. Li, Hierarchical microstructure design to tune the mechanical behavior of an interstitial TRIP-TWIP high-entropy alloy, Acta Materialia, 163, 2019, 40-54.
7. U. Chakkingal, A. Suriadi, P. Thomson, The development of microstructure and the influence of processing route during equal channel angular drawing of pure aluminum, Mater. Sci. Eng. A, 266, 1999, 241-249.
8. W.-J. Cheng, C.-J. Wang, Study of microstructure and phase evolution of hot-dipped aluminide mild steel during high-temperature diffusion using electron backscatter diffraction, Applied Surface Science, 257, 2011, 4663-4668.
9. Polyakova, A. Gulin, D. Constantinov, Investigation of microstructure and mechanical properties of carbon steel wire after continuous method of deformational nanostructuring, Appl. Mechan. Mater., 436, 2013, 114-120.
10. R. Mythili, R.K Irana, L. Herojit Singh, R. Govindaraj, A. Sinha, M. Singh, S. Saroja, M. Vijayalakshmi, M. Deb, Identification of Retained Austenite in 9Cr-1.4W-0.06Ta-0.12C Reduced Activation Ferritic Martensitic Steel, Symmetry, 14, 2, 2022, 196.
11. O. Kaibyshev, R. Kaibyshev R., G. Salishchev, Formation of submicrocrystalline structure in materials during dynamic recrystallization, Materials Science Forum. 113-115, 1993, 423-428.
12. J.Y. Huang, Y.T. Zhu, H. Jiang, T.C. Lowe, Microstructures and dislocation configurations in nanostructured Cu processed by repetitive corrugation and straightening, Acta materialia, 49, 9, 2001, 1497-1505.
13. Y. Saito, H. Utsunomiya, N. Tsuji, T. Sakai, Novel ultra-high straining process for bulk materials-development of the accumulative roll-bonding (ARB) process, Acta materialia, 47, 2, 1999, 579-583.
14. N. Tsuji, Y. Saito, S. Lee, Y. Minamino, ARB (Accumulative Roll-Bonding) and other new Techniques to Produce Bulk Ultrafine Grained

Materials, Advanced Engineering Materials, 5, 5, 2003, 338-344.
15. P.W. Bridgman, Effects of high shearing stress combined with high hydrostatic pressure, Physical Review, 48, 10, 1935, 825-847.
16. A.P. Zhilyaev, T.G. Langdon, Using high-pressure torsion for metal processing: Fundamentals and applications. Prog. Mater. Sci., 53, 2008, 893-979.
17. Y. Beygelzimer, D. Orlov, V. Varyukhin, A new severe plastic deformation method: Twist Extrusion, Ultrafine Grained Materials II. 2002, 297-304.
18. I. Volokitina, Structure and mechanical properties of aluminum alloy 2024 after cryo-genic cooling during ECAP, J. Chem. Technol. Metall., 55, 3, 2020, 580-585.
19. S. Lezhnev, I. Volokitina, T. Koinov, Research of influence equal channel angular pressing on the microstructure of copper, J. Chem. Technol. Metall., 49, 6, 2014, 621-630.
20. R.Z. Valiev, R.K. Islamgaliev, I.V. Alexandrov, Bulk nanostructured materials from severe plastic deformation, Prog. Mater. Sci., 45, 2000, 103-189.
21. D.P. Verma, Sh.A. Pandey, A. Bansal, Sh. Upadhyay, N.K. Mukhopadhyay, G.V.S. Sastry, R. Manna, Bulk Ultrafine-Grained Interstitial-Free Steel Processed by Equal-Channel Angular Pressing Followed by Flash Annealing, J. Mater. Eng. Perform., 25, 2016, 5157-5166.
22. A. Naizabekov, I. Volokitina, Effect of the Initial Structural State of Cr-Mo High-Temperature Steel on Mechanical Properties after Equal-Channel Angular Pressing, Phys. Met. Metallogr., 120, 2019, 177-183.
23. R. Pippan, S. Scheriau, A. Taylor, Saturation of fragmentation during severe plastic deformation, Annual Review of Materials Research, 40, 2010, 319-343.
24. A.V. Polyakov, I.P. Semenova, G.I. Raab, Peculiarities of ultrafine-grained structure formation in Ti Grade-4 using ECAP-Conform, Advanced Materials Science, 31, 1, 2012, 78-84.
25. A. Naizabekov, S. Lezhnev, E. Panin, I. Volokitina, A. Arbuz, T. Koinov, I. Mazur, Effect of Combined Rolling–ECAP on Ultrafine-Grained Structure and Properties in 6063 Al Alloy. Journal of Materials Engineering and Performance, 28, 2019, 200-210.
26. I. Volokitina, N. Vasilyeva, R. Fediuk, A. Kolesnikov, Hardening of Bimetallic Wires from Secondary Materials Used in the Construction of Power Lines, Materials, 15, 2022, 3975.
27. E.I. Fakhretdinova, G.I. Raab, R.Z. Valiev, Modeling of Metal Flow during Processing by Multi-ECAP-Conform, Advanced Engineering Materials, 17, 12, 2015, 1723-1727.
28. I. Volokitina, E. Siziakova, R. Fediuk, A. Kolesnikov, Development of a Thermomechanical Treatment Mode for Stainless-Steel Rings, Materials, 15, 2022, 4930.
29. V.A. Kuzmenko, Fatigue tests at high frequencies of loading. Kiev: Naukova Dumka, 1979, 335, (in Russian).
30. BY МПК G 01, 2009.